SOLAR ERUPTIONS AND LONG WAVELENGTH RADIO BURSTS: THE 1997 MAY 12 EVENT

N. Gopalswamy[1] and M. L. Kaiser[2]

[1]Center for Solar Physics and Space Weather, Department of Physics, The Catholic University of America, Washington DC 20064, USA

[2]NASA Goddard Space Flight Center, Greenbelt MD 20771 USA

ABSTRACT

We report on the cause of the 1997 May 12 type II bursts observed by ground based and space-based radio instruments. We estimate the fast mode speed in the corona as a function of heliocentric distance to identify the regions where fast mode shocks can be driven by CMEs. We find that both the coronal and the interplanetary type II bursts can be explained by shocks driven by the same CME at two different spatial domains. The fast mode speed in the corona has a peak at a heliocentric distance of $\sim 3\ R_\odot$ which does not allow the coronal shock wave to propagate beyond this distance. When the CME continues to travel beyond the fast mode peak, another shock forms in the interplanetary medium where the fast mode speed falls sufficiently. From the radio observations we can infer that the plane of the sky speed of the CME is smaller than the space speed by at least a factor of 2, consistent with the location of the eruption at N21 W08. The inferred CME speed is also consistent with previous deprojected speed estimates.

INTRODUCTION

Long wavelength radio bursts in the decameter-hectometric (DH) regime represent an effective diagnostic of solar disturbances leaving the Sun. Radio type II bursts are produced by MHD fast mode shocks (Gopalswamy et al. 2000c) at the local plasma frequency and its harmonic in the corona and interplanetary (IP) medium. By combining meterwave observations from the ground and DH observations from space, it is possible in principle to track some of these shocks through the entire Sun-Earth connected space. In practice, however, the correspondence between meterwave and DH has been very complex and poorly understood (Gopalswamy et al, 1998; Cliver et al., 1999; Reiner and Kaiser, 1999). While every DH type II burst is associated with a CME (Gopalswamy et al. 2000b) as in the case of kilometric type II bursts, many of them are not associated with metric type II bursts. Statistical studies have shown poor correlation between IP shocks detected *in situ* and those inferred from metric type II bursts (Gopalswamy et al., 2000c), probably due to the complex profile of the fast mode speed in the corona. Thus, a careful examination of the coronal and IP type II bursts along with the associated coronal mass ejection (CME) is necessary to understand their relationship. In this paper, we explore the relationship between coronal and DH type II bursts during the 1997 May 12 solar eruption, one of the first major events during the rising phase of cycle 23. Various aspects of this event such as Hα flare (Jain et al., 1997), white light CME (Plunkett et al., 1998), EUV transient (Thompson et al. 1998) and magnetic cloud at 1 AU (Webb et al., 2000) have already been reported.

OBSERVATIONS

The May 12, 1997 eruption involved both an active region (AR 8038, N21 W08) and its associated filament from the northwest quadrant of the Sun, resulting in a full-halo CME and an EUV transient observed by the Solar and Heliospheric Observatory (SOHO). The eruption also resulted in radio bursts in the metric, DH

Table 1. Time-line of the 1997 May 12 Solar Eruptive Event

Time (UT)	Activity
04:34	Loop Brightening following an Earlier Dimming
04:35	Projected onset time of EIT Wave
04:42 to 05:26	GOES C1.3 X-ray Flare from AR 8038, peak at 04:55 UT
04:50	Global Enhancement in EUV
04:54 to 05:03	Fundamental Metric type II burst
04:54 to 05:10	Harmonic Metric type II burst
04:57 to 05:18	Shock-associated type III bursts
05:06 to 05:15	DH type II (Fundamental)
05:10 - 06:04	Metric type IV burst
06:30	Leading edge of the LASCO CME at 3 $R_\odot$
12:00 on 05/14	Kilometric type II burst
01:00 on 05/15	Interplanetary shock detected by Wind
10:00 on 05/15	Magnetic Cloud detected by Wind

and kilometric domains. The DH and kilometric observations were made by the Wind/WAVES experiment (Bougeret et al., 1995). Table 1 shows a timeline of the event, starting from $\sim$ 04:34 UT on May 12, 1997.

Type II Bursts

The metric type II burst had fundamental (F) and harmonic (H) components staring at 04:54 UT, roughly about 10 min after the onset of the GOES X-ray flare. Radio spectra obtained by the Hiraiso Radio Spectrograph (HiRAS) shows that the starting frequency of the F-component was $\sim$ 60 MHz and continued to frequencies below 25 MHz. The H-component started at $\sim$ 120 MHz and ended at 30 MHz at 05:10 UT, within the observing frequency range of HiRAS (see Figure 1). The F-component continued into the Wind/WAVES dynamic spectrum for a short while and ended at 05:15 UT at a frequency of 10 MHz (see Figure 2). In three minutes, the F-component seems to have drifted from 25 MHz to 14 MHz. There were intense type III bursts, starting at 04:57 UT and ending shortly after the end of the DH type II burst. These type III bursts clearly start after the onset of the metric type II burst suggesting that they are due to shock-accelerated electrons. Taken together, the metric and DH dynamic spectra suggest that a type II shock existed between 60 and 10 MHz plasma levels.

After a long gap of more than a day, a kilometric type II burst started at 140 kHz. Since the eruptive event was sufficiently well isolated, we are confident that the kilometric type II burst was associated with the May 12, 1997 eruption. Following the kilometric type II burst, an IP shock was detected at 01:00 UT on May 15, 1997 by Wind's *in situ* plasma and magnetic field instruments (see e.g., Webb et al., 2000). The IP shock was clearly driven by an IP ejecta. From *in situ* measurements we found that the IP ejecta had an average speed of $\sim$ 450 km s^{-1} and lasted for $\sim$ 17 hr (Gopalswamy et al., 2000a).

White Light and EUV Observations

The earliest near-surface activity was an EUV loop brightening at $\sim$ 04:34 UT (Gopalswamy and Thompson, 2000) in the active region. A wave transient was observed by SOHO's Extreme-ultraviolet Imaging Telescope (EIT), moving away from the eruption site with a speed of $\sim$ 245 km s^{-1} (Thompson et al., 1998). The height-time plot of the EIT transient, when extrapolated to earlier times, coincided with the EIT loop brightening. The white light CME first appeared above the LASCO/C2 occulting disk at 06:30 UT with a sky-plane speed of $\sim$ 275 km s^{-1}, similar to the EIT transient speed. The white light speed of the CME was obtained by tracking the fastest part of the halo CME. Others have reported slightly different speeds for this event (Plunkett et al., 1998; Sheeley et al., 1999). The EUV transient and white light CME have similar speeds in the sky plane and their onset clearly precedes the associated flare. A global enhancement was observed in the EUV images at 04:50 UT, which was roughly symmetric around the region of eruption, and had a diameter of $\sim$ 10 arcmin. Global enhancement is a recently discovered phenomenon, which seems
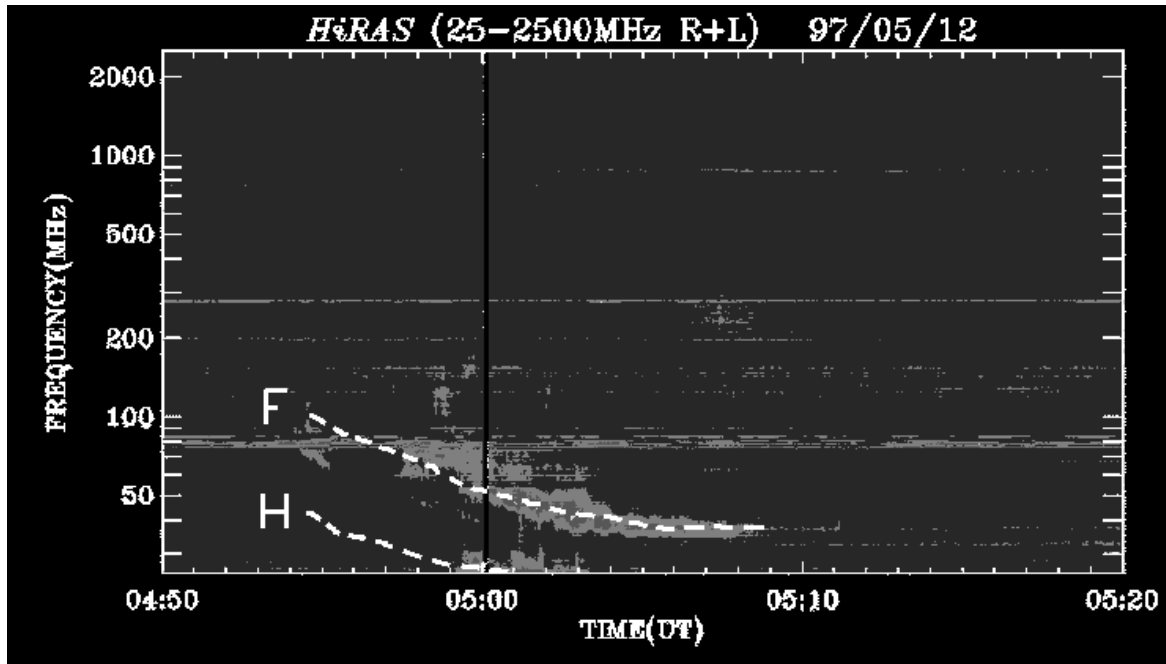
Figure 1: Dynamic spectrum obtained by the Hiraiso Radio Spectrograph (HiRAS) showing the fundamental (F) and harmonic (H) components of the metric type II burst. Some sections of the burst were weak, so we have drawn dashed lines through the components to guide the eye. The H-component ends within the HiRAS spectral range. The F-component continues to frequencies below the low frequency end of HiRAS.
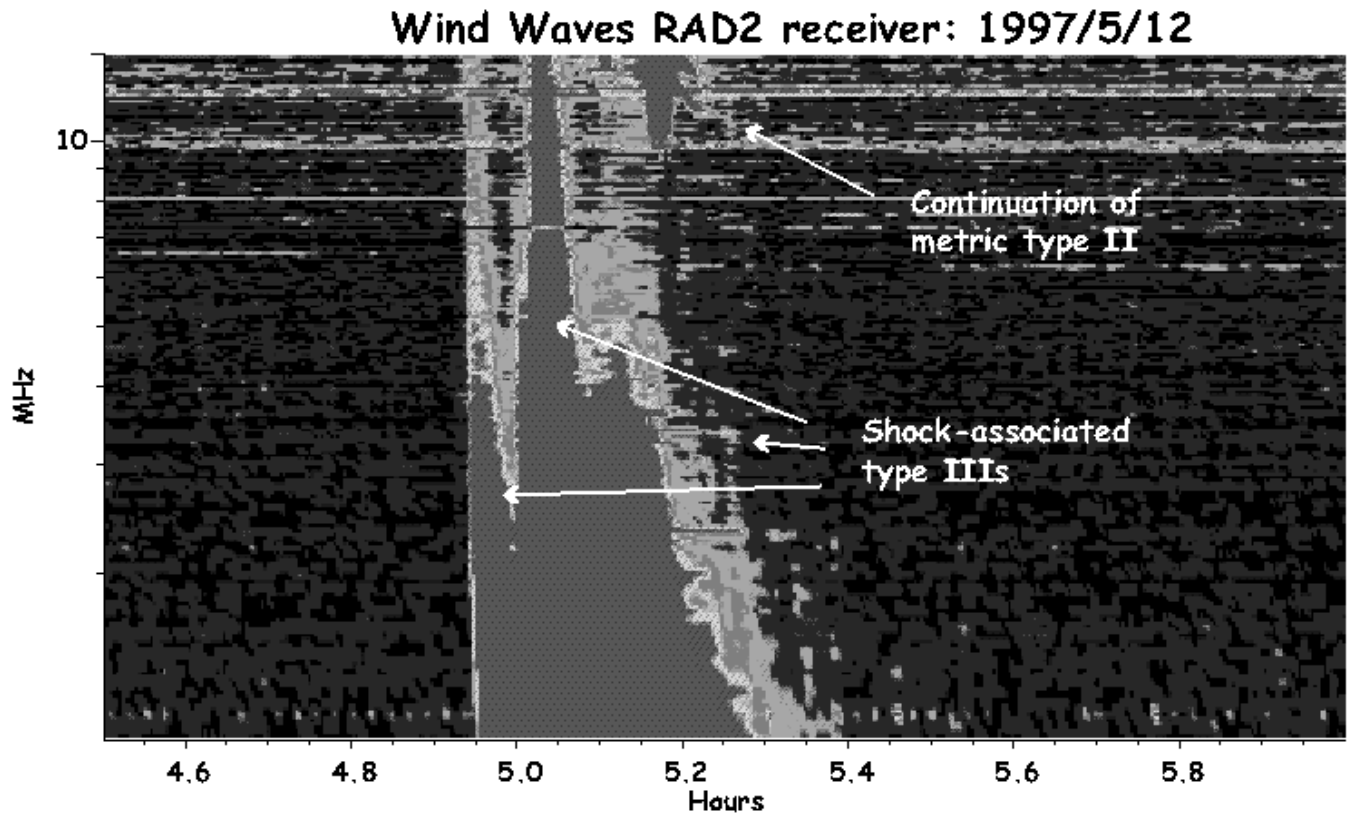

Figure 2: Dynamic spectrum in the DH domain (1-14 MHz) obtained by the Wind/WAVES experiment showing the continuation of the fundamental component of the metric type II burst and a series of intense type III bursts associated with the type II shock.

to be the earliest EUV signature of CMEs (Gopalswamy et al, 1999; 2000b). The most prominent and long-lasting EUV feature associated with the CME is the twin-dimming located to the north and south of the active region. Webb et al., (2000) interpreted that the feet of the CME flux rope are located in the EUV dimming regions. From Figure 1 of Webb et al. (2000) we see that the global enhancement clearly precedes the twin-dimming. We can reconcile the dimming and global enhancement as follows: If the flux rope is the expanding coronal coronal cavity, then the global enhancement may be the frontal structure of the CME.

ANALYSIS

Assuming a hemispherical shape for the eruption, one can estimate the heliocentric distance of the CME from the EUV global brightening as ~ 1.3 $R_\odot$ at 04:50 UT. The metric type II burst starts a few minutes later at 04:54 UT. We assume that the shock is formed at this time. If the CME is the shock driver, it must have attained a speed greater than the local fast mode speed (V_f) at this time. Figure 3 shows a plot of V_f as a function of radial distance for the quiet corona assuming a 3 × Saito model (Saito et al., 1977). Also plotted are the fundamental and harmonic frequencies (curves 1 and 2 in Figure 3) as a function of radial distance. Sections of curves 1 and 2 are thickened to show the frequency range over which the type II burst occurred in the metric and DH domains. For the density model used, the 60 MHz plasma level is at a distance of 1.5 $R_\odot$. Assuming that the CME originated from close to surface at 04:34 UT, it must have taken ~ 20 min to attain the fast mode speed. The type II burst ends at 05:15 UT when the CME must have lost the shock because V_f has increased considerably. Note that the type II burst ends at the 10 MHz plasma level (in the Wind/WAVES domain), corresponding to the region of peak fast mode speed (V_{fmax}). Thus we infer that the shock was able to survive only for the duration of the type II burst in the metric and DH domains.

Since there was an IP shock indicated by the kilometric type II burst and *in situ* observations, the CME must have started driving another shock in the IP medium. When exactly the IP shock started depends on the profiles of V_f and V_{sw} (the solar wind speed) in the IP medium. In the presence of the solar wind flow, the CME speed in excess of V_{sw} must exceed V_f to drive a shock. The Thermal Noise Receiver (TNR) of WAVES measured a plasma frequency of 45 kHz in the upstream of the shock as it arrived at Wind. For an inverse-square density dependence, assuming harmonic plasma emission, we infer that the kilometric type II burst must have started at a heliocentric distance of ~ 140 $R_\odot$ (0.65 AU).

The above analysis suggests that the CME speed has a lower limit, close to the local V_f in the heliocentric distance range 1.5 to 2.9 $R_\odot$. This limit is ~ 320 to 520 km s^{-1} (see the profile of V_f between the two vertical lines in Figure 3). When the type II burst ended, the CME probably had a speed of ~ 520 km s^{-1}. The CME speed, however, had to be lower than V_{fmax} as there was no radio emission at frequencies below 10 MHz. The inferred CME speed at 2.9 $R_\odot$ is thus almost twice as large as the plane of the sky speeds measured in EUV and white light images and is consistent with the deprojected speed obtained by Plunkett et al. (1998).

DISCUSSION AND CONCLUSIONS

A combined analysis of multiwavelength and multi-instrument data has helped us identify the shocks driving the type II bursts. First of all, the type II radio burst in the metric and DH domains is the same event, unlike in some cases where there is no obvious connection in the two domains. A similar event, a purely CME-driven metric type II burst that continued into the DH domain was reported by Gopalswamy (2000). Assuming that the shock was driven by the CME we found that the CME must have had a speed of at least 520 km s^{-1} when it reached ~ 2.9 $R_\odot$. If this is true, then the low sky plane speed is due to projection effects. The CME originated from close to the central meridian (N21 W08) and hence we expect significant projection effects. The higher CME speed is also consistent with the *in situ* speed (~ 450 km s^{-1}) which clearly exceeded the solar wind speed (~ 320 km s^{-1}).

An alternative interpretation for the type II shock would be a blast wave from the associated flare. The blast wave is expected to be super-Alfvenic during 04:54 to 05:15 UT and die off near the peak of the fast
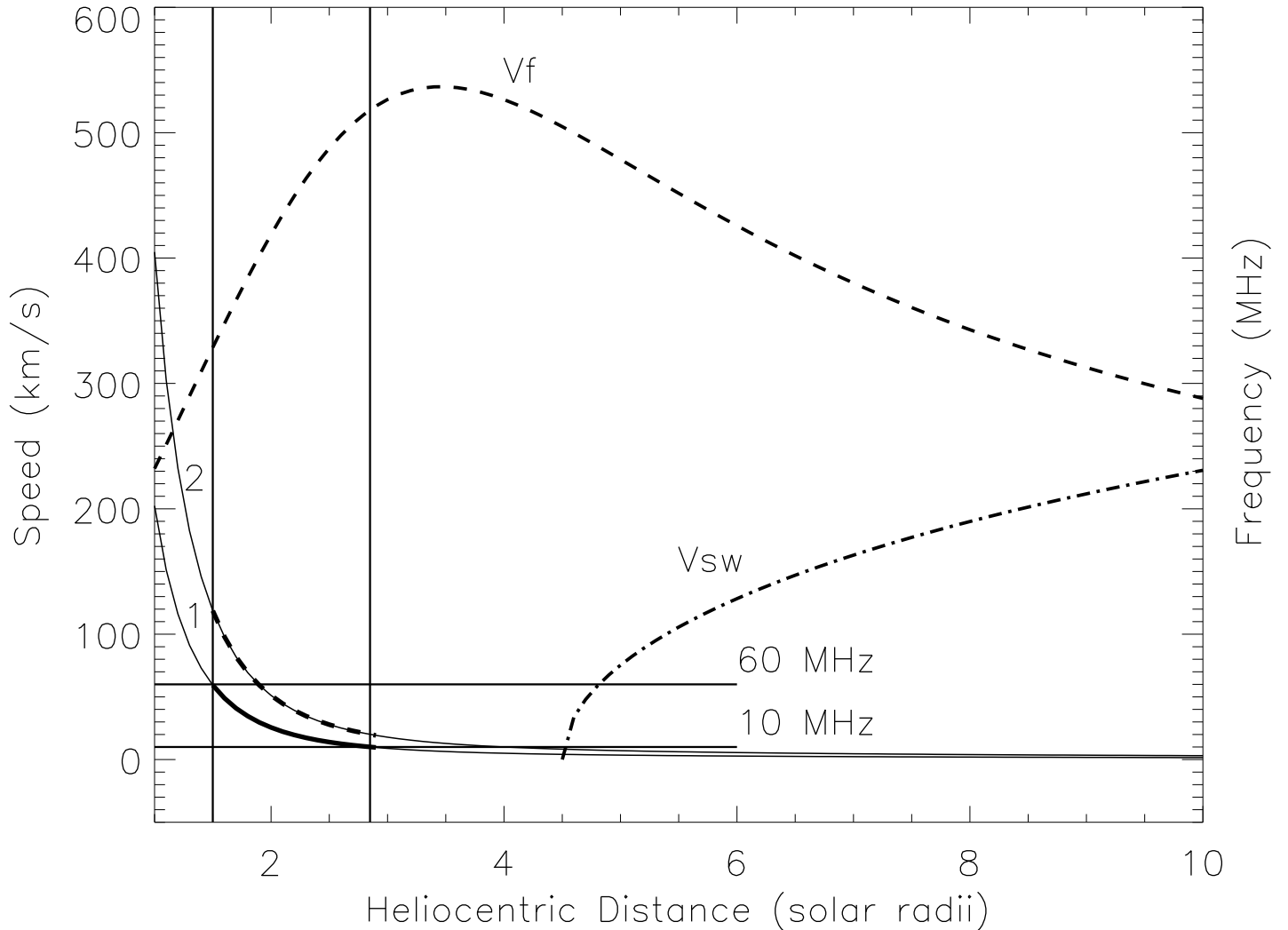
Figure 3: Plots of fast mode speed (V_f – dashed curve), solar wind speed (V_{sw} – dot-dashed curve), fundamental (curve 1) and harmonic (curve 2) plasma frequencies as function of heliocentric distance in solar radii ($R_\odot$). The two vertical lines at 1.5 and 2.85 $R_\odot$ represent coronal layers where the the type II burst started and ended while the two horizontal lines (60 MHz and 10 MHz) mark the corresponding plasma levels. The plasma frequency curves bounded by the pairs of horizontal and vertical lines represent the frequency domain of the fundamental and harmonic type II bursts as derived from the HiRAS dynamic spectrum. Curves 1 and 2 are thickened by solid and dashed curves to indicate the radio burst. Note the peak in V_f around 3 $R_\odot$.

mode speed (see Figure 3). In this case, the DH type II burst also has to be due to the blast wave. In this scenario, the CME would have slowly accelerated and become super-Alfvenic only in the IP medium to produce the kilometric type II burst. While we cannot rule out the blast wave scenario, we prefer the CME-driven scenario because of the relatively low starting frequency of the metric type II burst and its continuation into the DH domain. This is also consistent with the profuse DH type III bursts when the CME arrives at the plasma level corresponding to the DH domain.

In a related study, Mann et al. (1999) obtained a speed of 1029 km s^{-1} for the coronal shock assuming one-fold Newkirk model for the coronal density. This is much larger than all the mass motions observed during this event. According to these authors, the EIT wave and the coronal shock are generated in the same flare such that the EIT wave represents the pre-shock stage of the fast mode wave in the lower corona, which eventually steepens to become the shock. This interpretation is similar to the blast wave scenario. Mann et al. (1999) obtained an Alfven wave speed profile which peaks at ~ 800 km s^{-1}. Since the inferred speed of the coronal shock is 1029 km s^{-1}, the coronal type II bursts should have continued for several solar radii more, contrary to the observations. In conclusion, the coronal and interplanetary type II radio bursts associated with the May 12 1997 CME can be interpreted as due to two shocks one near the Sun and the other far into the IP medium due to a complex interrelationship of the CME speed, the fast mode speed and the solar wind speed. The ambient conditions ahead of the CME were favorable for shock formation in two stretches in the space between Sun and Earth.

ACKNOWLEDGEMENTS

REFERENCES

Bougeret, J.-L. et al., *Space Sci. Rev.*, 71, 231, (1995)

Cliver, E. W., Webb, D. F. and Howard, R. A., *Solar Phys.*, 187, 89, (1999)

Gopalswamy, N., in Radio Astronomy at Long Wavelengths, eds. R. G. Stone, K. W. Weiler, M. L. Goldstein, and J.-L Bougeret, Geophysical Monograph 119, p. 123, (2000)

Gopalswamy, N. et al., *JGR*, 103, 307, (1998)

Gopalswamy, N., Nitta, N., Manoharan, P. K., Raoult, A. and Pick, M., *Astron. Astrophys.*, 347, 684, (1999)

Gopalswamy, N. and Thompson, B. J., *JASTP*, 62(16), 1457, (2000)

Gopalswamy, N. et al., *GRL*, 27, 145, (2000a)

Gopalswamy, N. et al., *GRL*, 27, 1427, (2000b)

Gopalswamy, N., Lara, A., Kaiser, M. L. and Bougeret, J.-L., *JGR*, in press, (2000c)

Jain, R. et al., in Correlated Phenomena at the Sun, in the Heliosphere and in Geospace, ESA SP-415, p. 145, (1997)

Mann, G., Aurass, H., Klassen, A., Estel, C., and Thompson, B. J., *ESA SP-446*, p. 477, (1999)

Plunkett, S. P. et al., *GRL*, 25, 2477, (1998)

Reiner, M. J. and Kaiser, M. L., *JGR*, 104, 16979, (1999)

Saito, K., Poland, A. I. and Munro, R. H., *Solar Phys.*, 55, 121, (1977)

Sheeley, N. R., Jr., Walters, J. H., Wang, Y.-M., Howard, R. A., *JGR*, 104, 24,739, (1999)

Thompson, B. J. et al., *GRL*, 27, 2465 (1998)

Webb, D. F. et al., *JGR*, 105, 27251, (2000)